

Improvement of Thermoluminescence Properties of α - Al_2O_3 Using Metallic Dopants for Dosimetry Application

Mohammad Reza Jalali^{1*}

¹ Department Of Physics, Payame Noor University; P.O.Box 19395-4697, Tehran, Iran

* CORRESPONDENCE: ✉ mrjalali93@yahoo.com

ABSTRACT

In this study, dosimetric phosphor, α - Al_2O_3 nanopowder was prepared using the soluble combustion method and its thermoluminescence (TL) characteristics were analyzed. In order to improve thermoluminescence properties of α - Al_2O_3 , the nanopowder was doped with Mg and Li, transition metals and was annealed. Structural and morphological characteristics of synthesized α - Al_2O_3 :Mg,Li nanopowder phosphor were identified via X-ray Diffraction, Scanning Electron Microscopy. Finally, thermoluminescence properties of the α - Al_2O_3 nanopowder, doped with different amounts of Mg (0.2 wt% - 0.8wt%) and Li (0.5wt%-1.5wt%) were studied. The best thermoluminescence effect was achieved via the co-doped of Mg and Li in α - Al_2O_3 nanopowder. X-rays analysis determined that the crystalline structure of the synthesized Mg and Li doped α - Al_2O_3 was completely consistent with α - Al_2O_3 crystalline structure. Also, TL analysis showed that after thermal annealing, some peaks of curves disappear. The sample of α - Al_2O_3 :Mg0.4%,Li1% had the strongest peak after the annealing. For synthesis of α - Al_2O_3 samples by solvent-combustion method, the raw material of $(\text{Al}(\text{NO}_3)_3 \cdot 9\text{H}_2\text{O})$ and $(\text{H}_4\text{N}_2\text{CO})$ were used. In addition to the abovementioned materials, LiNO_3 and $\text{Mg}(\text{NO}_3)_2$ were also used to prepare the doped specimens.

Keywords: thermoluminescence behavior, Solution Combustion Synthesis (SCS), aluminum doped lithium oxide, aluminum doped manganese oxide, dosimetry

INTRODUCTION

Nowadays, Thermoluminescence is used in three main areas: geological history, archaeological age and radiation dosimetry. The third one is the most important area and thermoluminescence is widely used in this area. The use of thermoluminescence is to determine the amount of radiation that a person has exposed to in the workplace or due to medical treatments for cancer treatment. In personal dosimeter, the employee was equipped with a thermoluminescence machine called dosimeter. This dosimeter is the amount of radiation that the person is exposed to it, which should be measured periodically. If the amount of radiation exceeds the permissible limit, the presence of a person in that environment is dangerous and should be distant from that environment for a while. Work environments that are hazardous to these dangers and should use dosimeters include nuclear stations and radiotherapy departments in hospitals. In addition, monitoring the amount of radiation that a patient is exposed to is also important. For this purpose, dosimeters (which took place inside the body) have been developed and successfully supervised the treatment. Aluminum oxide (Al_2O_3) is one of the first study materials which used as a dosimeter. Although the study on these substances was forgotten for a long time, due to their low sensitivity compared to the 100-TLD (LiF:Mg,Ti), but recently, the study on these substances has increased due to the progression of crystals $\text{Al}_2\text{O}_3\text{:C}$.

Article History: Received 12 January 2018 ♦ Revised 23 April 2018 ♦ Accepted 15 May 2018

© 2018 The Author(s). Open Access terms of the Creative Commons Attribution 4.0 International License (<http://creativecommons.org/licenses/by/4.0/>) apply. The license permits unrestricted use, distribution, and reproduction in any medium, on the condition that users give exact credit to the original author(s) and the source, provide a link to the Creative Commons license, and indicate if they made any changes.

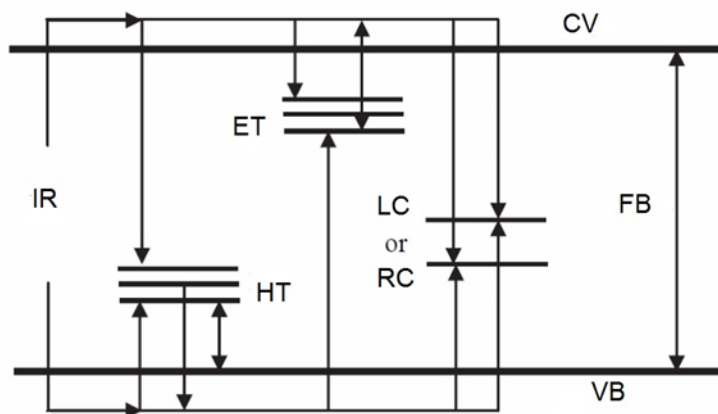


Figure 1. Mechanism of thermoluminescence process in a semiconductor

Thermoluminescence

The luminescence mechanism in semiconductors has at least two stages: (1) Ionizing Radiation (IR), which is due to both the Electron Traps (ET) and the Hole Traps (HT); (2) the electrons and free-carriers that are produced in the Conduction Band and the Valence Band. Thermoluminescence is the thermal irradiation of light resulting from the previous absorption of energy from ionizing radiation obtained from an insulator or semiconductor. The thermoluminescence process can be realized based on the structural model of semi-conductive bands. In a semiconductor, there are two important energy bands: (1) an almost full valence band and (2) an almost empty conduction band. These two energy bands are separated with a forbidden band gap, which means that there is no level of electron energy between these two bands. The transfer of electrons between the valence band and the conduction band is allowed, so that it produces free electrons in conduction band and free holes in valence band. The energy difference between the two bands is determined by the energy of gap band (see **Figure 1**).

Due to ionizing radiation, electrons are transferred from the valence band to the conduction band, which results in the production of a significant amount of free electrons (in the conduction band) and free holes (in the valence band); in this case, electron-hole pairs are created. To keep the crystal electron neutral, a hole is created for each electron that gets trapped inside the electron traps. These holes may also be trapped inside the other traps. During irradiation, electrons and free holes can move inside the crystal, as long as they are trapped by impurities, luminescence centers and other imperfections in the crystal. The electrons and holes are then re-distributed continuously in the electronic traps and the hole traps. After irradiation, trapped electrons and holes can be released. This is done by heating the crystal to medium temperatures (optimal amount of heat energy), which coincides with the passage of a particular energy potential barrier.

Combustion Synthesis

Considering the significant increase in demand for alumina ceramics, especially Al_2O_3 , as well as the inability of the traditional Bayer process to produce high-surface Al_2O_3 powder, several chemical methods were suggested including precipitation, spray pyrolysis, sol-gel, organic precursors, Pechini and etc. However, these methods require complicated and time-consuming technique. This is an obstacle to repeatability, low cost and high reliability for final powders. In addition, in these methods, α - Al_2O_3 powder is obtained after annealing of different precipitates at a temperature higher than 1100°C . The solution combustion synthesis (SCS) method is a solution for some of the aforementioned problems which have attracted many researchers in recent years. Combustion synthesis involves an exothermic reaction among an oxidizing agent such as nitrate of metals, ammonium nitrate and Ammonium perchlorate, and an organic fuel such as urea ($\text{CH}_4\text{N}_2\text{O}$), carbonylhydrazide ($\text{CH}_6\text{N}_4\text{O}$), and glycine ($\text{C}_2\text{H}_5\text{NO}_2$).

The combustion reaction occurs in a muffle furnace or on a hot plate at a temperature of 500°C or less, which is at a very lower temperature than the fuzzy temperature of the target material. In typical reactions, a primary solution of water, nitrate of metals and fuel, decomposes and then dehydrates and eventually ignites. The resulting product is a bulky foam powder that occupies the entire volume of the sintering crucible. Without any external heat source, the chemical energy liberated from the exothermic reaction between the

metal and fuel nitrates can quickly bring the system to high temperatures (over 1600 °C). The combustion synthesis powders are more homogeneous than conventional solid state methods, with fewer impurities and more surface area. The combustion reaction mechanism is relatively complicated. The parameters that affect the reaction include fuel type, the ratio of fuel to oxidizer, use of additional oxidizing agents, combustion temperature, and the amount of water of the original mixture. In general, an appropriate fuel should not act very severe and produces toxic gases. When the reaction occurs completely, the only gases that are produced are N₂, CO₂ and H₂O, which makes it an environmentally friendly method. The most important advantages of this process are (1) low energy requirements (does not require additional annealing), (2) Saving time (the whole process is done in just a few minutes), and (3) being environmentally friendly (Combustion reaction products include: N₂, CO₂ and H₂O). Many researchers have reported the formation of single-phase α-Al₂O₃ powder (using urea, carbonylhydrazide, and hydrazine) as fuel and without any subsequent heat treatment. At the same time, other researchers reported that glycine, or citric acid, produced amorphous powder which converts to α-Al₂O₃ after annealing above 1100 °C, which in this case, the formation of α-Al₂O₃ occurs after the formation of the middle phase of γ-Al₂O₃. According to the aforementioned mechanisms for thermoluminescence, creating structural defects in α-Al₂O₃ is a way to increase thermoluminescence properties. This is done using various impurities as dopant. In this paper, lithium and magnesium impurities were used to improve the α-Al₂O₃ thermoluminescence properties. To produce pure α-Al₂O₃ and also to import impurities into its crystalline structure, we used the SCS method, which is a low-cost and affordable way.

RESEARCH METHODS

Doped and un-doped samples of α-Al₂O₃ were synthesized as follows using soluble combustion synthesis methods:

To prepare undoped samples, stoichiometric values of aluminum nitrate Al(NO₃)₃·9H₂O and H₄N₂CO (which is used as fuel) was dissolved based on Reaction 1 in the 50mL twice ionized water and placed on a magnetothermal heater at 50 °C and 360 rpm for 30 minutes. After 30 minutes, the temperature increased to 200 °C, and the solution was allowed to lose their water.



Then, what remained was poured into the alumina Crucible and transferred to the furnace. The furnace temperature was adjusted to 500 °C and the sample was allowed to be heated with furnace. The solution lost its water, foamed and then puffed, until near 400 °C, a rapid reaction with a large amount of visible gas and flame appeared, which, in fact, it was the same reaction as combustion. The reaction suddenly collapsed, and what remained was the white powder inside the crucible, that allowed it to be cool in the furnace to room temperature. Then the powder was collected and pound inside the mortar and was placed in an alumina crucible for annealing. The annealing process was also carried out in the tube furnace and in the air atmosphere. For this purpose, the powder was heated from the room temperature up to 1000 °C with 7 °C/min rate. It was kept for 2 hours at 1000 °C, then, it was cooled down to the room temperature in the oven. After that, the powder is removed from the crucible, and was pound inside the crucible again. A process similar to that described above was used to prepare the doped Al₂O₃ samples, with this different that the required dopant was added to the initial solution (dissolved inside the water). In this paper, LiNO₃ and Mg(NO₃)₂·3H₂O was used for the doping of lithium and Mg into the structure of alumina. The percentages of impurities used in this study were 0.5, 1 and 3% lithium and 0.2, 0.4 and 0.8% Mg, which were added to alumina. For simultaneous doping, a combination of 1% lithium and 0.4% Mg was used as a dopant. X-ray diffraction analysis (XRD) powder was studied using a PHILIPS PW1730 device. Powder morphology was also evaluated using scanning electron microscope (SEM) of TESCAN model. Samples were exposed to 1Gy gamma radiation with Co-source. Made Home TL Reader was used to read the irradiated samples. 60 Gamma Radiations with the Co-source of samples with 10 °C/min heat rate from 50 °C to 300 °C has been read.

RESULT AND DISCUSSION

The effect of dopant on the luminescence of ceramics can be explained through solid-state bond theory. This theory includes a solid insulating material with a prohibition gap, which has a semi-stable state, and when it is evoked, the electrons are trapped in it. Luminescence will be obtained if the lost energy is in the proper range of energy and wavelength, when the electrons leave the traps. There are several types of traps that can produce luminescence. Luminescence is called intrinsic, if the luminescence is produced by a structural defect that is characteristic of the mother network. Abnormal luminescence is another type of

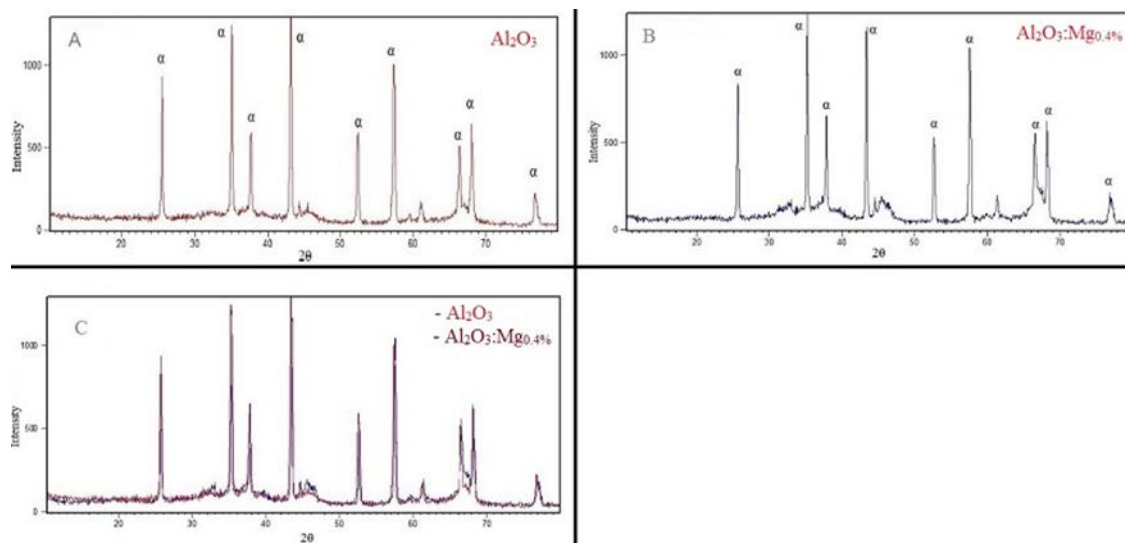


Figure 2. X-ray diffraction analyses; A) Analysis of pure alumina sample, B) Analysis of α - $\text{Al}_2\text{O}_3:\text{Mg}_{0.4\%}$, C) Comparison of A and B

luminescence caused by impurities in the structure. Impurities that can produce luminescence (and are usually used as dopants) are mainly intermediate elements, rare earth elements and actinides. The reason for this is the creation of electron capability in the orbital d or f. These impurities are the main source of luminescence in ceramics which are substituting within the structure of the mother network. Generally, the intensity and duration of the luminescence depends on the electron configuration of the activating ions and the nature of the mother's network, which includes activating ions. These dopants in luminescence materials increase luminescence efficiencies, which are sent to improve the synthesis of activating ions or improve the energy of the process. If we look at this from another aspect, adding a Dopant to the mother structure leads to distortions within the network. These disturbances create new trap centers, and as a result, when the substance is irradiated, the ability to amplify the electrons and the holes in it improves, and when the reading is done, it shows more intense peaks in its radiation curve. As a result, in this study we have used Mg (which is an intermediate element) to improve the thermoluminescence properties of alumina. We also used lithium as a common dopant in this study. **Figure 2** indicates the X-ray diffraction (XRD) results for pure α - Al_2O_3 and α - $\text{Al}_2\text{O}_3:\text{Mg}_{0.4\%}$ samples prior to the annealing process. In fact, one of the features of the SCS method is direct production of α - Al_2O_3 . However, the product in other methods is either amorphous or γ - Al_2O_3 , which should be converted to α - Al_2O_3 during an aniline stage. This issue illustrates the importance of the SCS method, which in fact can produce the desired product at a lower level. And as a result, it will be more cost-effective. **Figure 2-A** refers to the pure Al_2O_3 sample, that no impurity has been added to it. It can be seen that this graph fully corresponds to the α - Al_2O_3 graph.

Figure 2-B also describes the sample of $\text{Al}_2\text{O}_3:\text{Mg}_{0.4\%}$. As can be seen in **Figure 2**, this diagram is also consistent with the α - Al_2O_3 graph. It is also found in **Figure 2-C** that the X-ray diffraction patterns of α - Al_2O_3 and $\text{Al}_2\text{O}_3:\text{Mg}_{0.4\%}$ has a little difference, and they are match with each other. But with a little precision in the angles of the peaks, it can be seen that the peaks of the sample $\text{Al}_2\text{O}_3:\text{Mg}_{0.4\%}$ have somewhat shifted to the right. In **Figure 2**, the position of the peaks in relation to each other is clearly indicated. As you can see, the blue color chart is about $\text{Al}_2\text{O}_3:\text{Mg}_{0.4\%}$. It has shifted about 0.14 degrees to the right, which is due to a difference. In fact, this displacement in peaks is due to the formation of some residual stress in the doped sample. This is due to the difference in Atomic radius of Mg^{2+} and Al^{3+} . In fact, this displacement in the peaks is due to the formation of some amount of residual stress in the doped sample, which is also due to the replacement of Mg^{2+} ions with an ion radius of 0.73\AA instead of Al^{3+} with a 0.53\AA Atomic radius. In fact, placing an ion with a larger radius instead of a smaller radius ion causes some distortion and consequently a residual stress in the sample. Therefore, according to these documents, it can be concluded that using this method, magnesium ions have successfully entered (doped) into the crystalline structure of alumina. It will be seen later that this doping process will increase the thermoluminescence of nano-alumina. In the case of lithium-

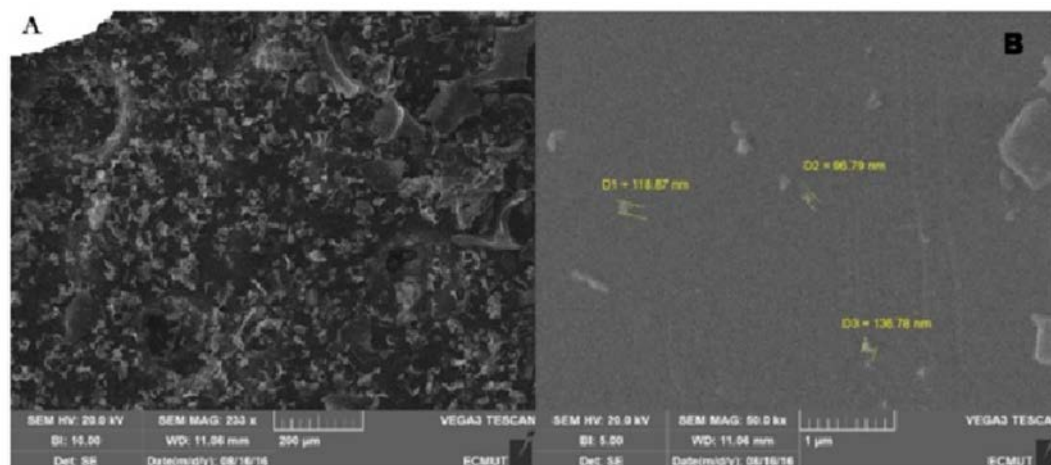


Figure 3. A) SEM image of α - Al_2O_3 sample with a magnification of 200 μm , B) SEM image of α - Al_2O_3 sample with a magnification of 1 μm , C) the EDS curve of α - Al_2O_3

doped specimens, same thing can be observed. The size of crystallites can be measured according to the XRD chart and the Scherrer relationship. This relationship is as follows:

$$t = k\lambda / \beta \cos \theta \quad (2)$$

where t is the amount of crystallite, k is a constant and equal to 0.9, λ is the wavelength of X-radiation, θ is diffraction angle, and β is the Full-Width Half-Maximum, or FWHM. By putting the numbers in the above formula, $t = 73.92\text{nm}$ will be obtained. Another feature of the SCS method is the production of nano-particle powders. The reason for the production of nanoparticles in the SCS method can be explained by the fact that the production of gas products increases the surface area of the powders by producing porous micro and nano porosity. The difference in particle size with the use of various fuels during combustion depends on the number of released molecules. So, when a fuel is used to produce an intense and effective combustion reaction, more gases are released, the agglomeration is split and more heat is transported by the system. And as a result, particle growth will be inhibited. Therefore, particles will be produced in the form of nanoparticles. **Figure 3** illustrates the SEM powder of pure alumina. **Figure 3-A** shows a smaller magnification and **Figure 3-B** shows a larger magnification of pure alumina powders. **Figure 3-C** indicates the EDS diagram of this sample, which is observed to fully correspond to the Al_2O_3 composition.

Reaction 1 indicates the stoichiometric reaction between $\text{Al}(\text{NO}_3)_3 \cdot 9\text{H}_2\text{O}$ and $\text{H}_4\text{N}_2\text{CO}$. As you can see, the product of this reaction is solid alumina and gas products include carbon dioxide, water vapor and nitrogen. If the reaction is done in full and efficient manner (i.e., due to lack of fuel or other factors), these gas molecules can cause nanoparticle production. As already mentioned, one of the ways to increase the thermoluminescence properties is to create structural defects in the α - Al_2O_3 domain. This is done using various impurities as a dopant.

The TL curve of the annealed samples was studied. There was no peak in the sample of pure α - Al_2O_3 samples; no doping was added to it. The results obtained from the analysis of samples containing magnesium and lithium impurities are presented in **Figure 4**. As shown in **Figure 4**, Example 1 has a peak at around 260°C, Sample 2 did not show any sign, Sample 3 has a peak at around 245°C, Sample 4 has a weak peak at around 190 °C, Sample 5 has a peak at around 197°C, and finally, Sample 6 has a weak peak at around 180°C.

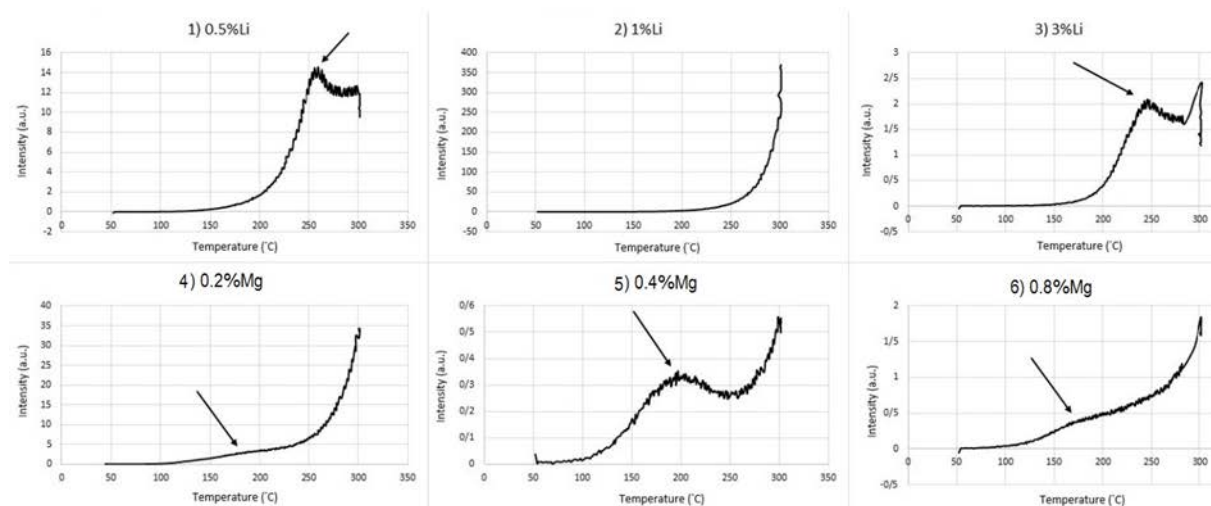


Figure 4. TL of 6 different samples 1) $\text{Al}_2\text{O}_3:\text{Li}_{0.5\%}$, 2) $\text{Al}_2\text{O}_3:\text{Li}_{1\%}$, 3) $\text{Al}_2\text{O}_3:\text{Li}_{3\%}$, 4) $\text{Al}_2\text{O}_3:\text{Mg}_{0.2\%}$, 5) $\text{Al}_2\text{O}_3:\text{Mg}_{0.4\%}$, 6) $\text{Al}_2\text{O}_3:\text{Mg}_{0.8\%}$ before annealing

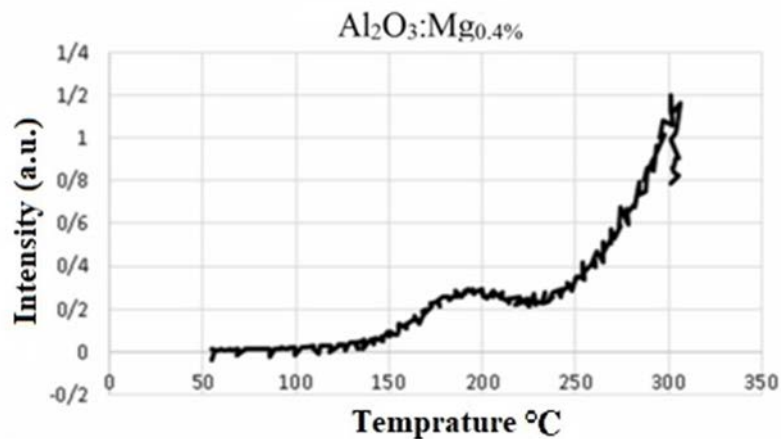


Figure 5. TL Radiation curve of $\text{Al}_2\text{O}_3:\text{Mg}_{0.4\%}$ which was annealed for 2 hours in 1000°C

Among the peaks shown in **Figure 4**, the peak of sample 5 has the best conditions, because firstly, a peak is completely distinct and secondly it appears at a favorable temperature. The characteristics of an optimal dosimeter are that its radiation curve has a single peak at a temperature of 200°C (180°C - 250°C). Considering this principle, doped samples with lithium are not suitable dosimeters before the annealing, because sample 2, which did not display a peak, and the peak of samples 1 and 3, also appeared at high temperatures. In the case of magnesium doped samples, it is suitable for the peak appearance of magnesium, but the problem is that the peaks appearing in sample 4 and 6 are very weak. But it is seen that sample 5 has a suitable peak.

Subsequently, the doped samples, which were annealed at 1000°C for 2 hours, were subjected to thermoluminescence analysis. According to the results, it was found that among the 6 samples presented in **Figure 4**, only sample 5, namely $\text{Al}_2\text{O}_3:\text{Mg}_{0.4\%}$, still have peak after the annealing. As shown in **Figure 5**, there is a peak at a temperature of 190°C in the radiation curve of this sample.

One of the main characteristics of a dosimeter is its ability to be anneal-able. It will not lose its properties after annealing, because sometimes it is necessary to make incremental readings. In this case, pre-radiation information must be completely erased before the process is repeated. In general, this is done with a heating process called "annealing". Magnesium is a suitable dopant for alumina, because when 0.4% magnesium is in the doped-alumina, it has a peak at an appropriate temperature before and after the annealing of the annealing curve.

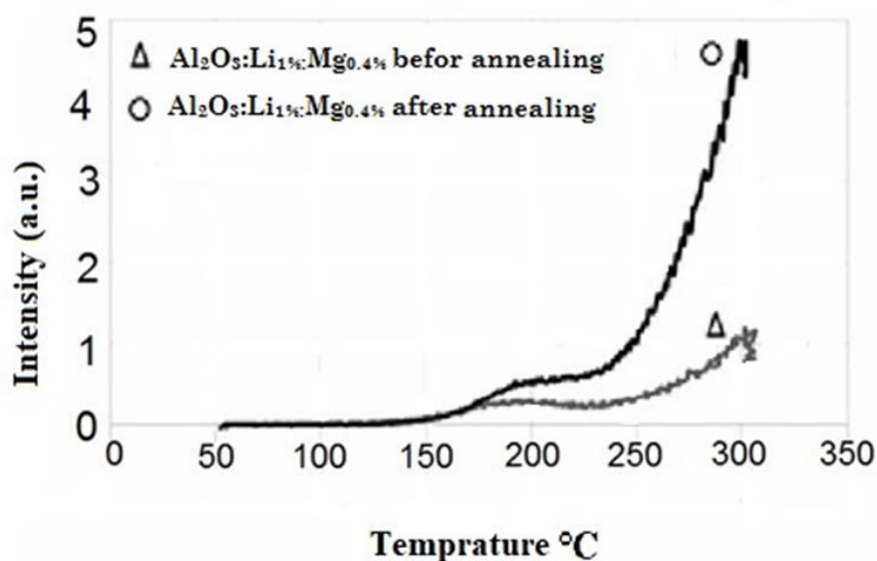


Figure 6. TL Radiation curves of $\text{Al}_2\text{O}_3:\text{Li}1\%:\text{Mg}0.4\%$ before and after annealing

Comparison of annealed and non-annealed samples indicated that the peaks of sample 1 and sample 3 with high emergence temperatures and peaks of samples 4 and 6, (which appeared at favorable temperatures but weak peaks) disappeared after the annealing.

In fact, in one direction, it can be said that all four pikes before the annealing were in an unstable condition and were removed after the annealing. The reason for this is not entirely clear, but it may be due to the release of the dopant from the inside of the alumina by the annealing process. Jun et al. (2005) found that C and Cr can be removed from the Al_2O_3 structure after annealing, which is also a reaction to oxygen and the oxidation process. It's likely that something like this has happened here. In samples where the amount of dopant, type of dopant, or a combination of both is not appropriate, the structure will be unstable and susceptible to the reaction, and since the annealing process has been carried out in the normal atmosphere, the conditions for the oxidation process have been provided. But the sample 5 is the only sample that has clear peaks and before the annealing, and also appears at an appropriate temperature of about 200°C .

Since the non-annealed samples were placed at a higher dose, comparing the intensity of the peak of this sample before and after the annealing which was provided in **Figures 4 and 5**, it can be concluded that this sample indicates a more intense peak after annealing, and as a result, the annealing process had a positive effect on it. Finally, to study the effect of simultaneous doping on the properties of thermoluminescence of alumina, a sample with 1wt % lithium and 0.4wt% of magnesium was synthesized. This sample showed no peak before the annealing, but after annealing, a peak appeared at a temperature of 200°C in its radiation curve. The reason for this can be explained as one of the effects of the annealing process on the stabilization of Electron Traps (ET) and the Hole Traps (HT). Possibly these traps were not stable before the annealing, and as a result, no peak was observed in the radiation curve, but after annealing, a peak appeared at a proper temperature in the radiation curve.

CONCLUSION

Thermoluminescence $\alpha\text{-Al}_2\text{O}_3$ nanopowder was synthesized using SCS method. The thermoluminescence properties of $\alpha\text{-Al}_2\text{O}_3$ was improved by doping Mg and Li, transition metals into the alumina structure.

Based on thermoluminescence analysis, it was found that after the annealing, only $\text{Al}_2\text{O}_3:\text{Mg}0.4\%$ and $\text{Al}_2\text{O}_3:\text{Li}1\%:\text{Mg}0.4\%$ samples had a thermoluminescence peak. The temperature of these peaks was also favorable and the peak intensity in sample $\text{Al}_2\text{O}_3:\text{Li}1\%:\text{Mg}0.4\%$ was higher than sample $\text{Al}_2\text{O}_3:\text{Mg}0.4\%$ which confirmed that simultaneous doping of Mg and Li resulted in higher increase in thermoluminescence properties of alumina.

Notes on contributors

Mohammad Reza Jalali – Department of Physics, Payame Noor University; P.O.Box 19395-4697, Tehran, Iran

REFERENCES

- Aboud, H., Saber, S., Wagiran, H., & Hussin, R. (2017). Energy response and thermoluminescence properties of lithium potassium borate Glass co-doped with Cu and SnO₂ nanoparticles. *Journal of Radiation Research and Applied Sciences*, 10(1), 1-5. <https://doi.org/10.1016/j.jrras.2014.12.009>
- Barrón, V. R. O., Ochoa, F. M. E., Vázquez, C. C., & Bernal, R. (2016). Thermoluminescence of novel MgO–CeO₂ obtained by a glycine-based solution combustion method. *Applied Radiation and Isotopes*, 117, 86-90. <https://doi.org/10.1016/j.apradiso.2016.02.002>
- Blair, M. W., Jacobsohn, L. G., Bennett, B. L., Tornga, S. C., Yukihiro, E. G., McKigney, E. A., & Muenchausen, R. E. (2009). Luminescence and structural properties of oxyorthosilicate and Al₂O₃ nanophosphors. *physica status solidi (a)*, 206(5), 904-909. <https://doi.org/10.1002/pssa.200881275>
- Doull, B. A., Oliveira, L. C., & Yukihiro, E. G. (2013). Effect of annealing and fuel type on the thermoluminescent properties of Li₂B₄O₇ synthesized by solution combustion synthesis. *Radiation Measurements*, 56, 167-170. <https://doi.org/10.1016/j.radmeas.2013.02.003>
- Escobar, O., Orante, B., Cruz, V., & Bernal, R. (2015). Thermoluminescence of magnesium oxide doped with cerium and lithium obtained by a glycine-based solution combustion method.
- Milliken, E. D., Oliveira, L. C., Denis, G., & Yukihiro, E. G. (2012). Testing a model-guided approach to the development of new thermoluminescent materials using YAG: Ln produced by solution combustion synthesis. *Journal of Luminescence*, 132(9), 2495-2504. <https://doi.org/10.1016/j.jlumin.2012.04.035>
- Oliveira, L. C., Yukihiro, E. G., & Baffa, O. (2016). MgO: Li, Ce, Sm as a high-sensitivity material for Optically Stimulated Luminescence dosimetry. *Scientific reports*, 6, 24348. <https://doi.org/10.1038/srep24348>
- Orante-Barrón, V. R., Escobar-Ochoa, F. M., Cruz-Vázquez, C., & Bernal, R. (2015). Thermoluminescence of novel zinc oxide nanophosphors obtained by glycine-based solution combustion synthesis. *Journal of Nanomaterials*, 16(1), 17. <https://doi.org/10.1155/2015/273571>
- Ozdemir, A., Yegingil, Z., Nur, N., Kurt, K., Tuken, T., Depci, T., & Yu, Y. (2016). Thermoluminescence study of Mn doped lithium tetraborate powder and pellet samples synthesized by solution combustion synthesis. *Journal of Luminescence*, 173, 149-158. <https://doi.org/10.1016/j.jlumin.2016.01.013>
- Rai, R. K., Kher, R. S., Dhoble, S. J., Divya, N., & Upadhyay, A. K. Synthesis and Luminescence Characterization of Eu Activated Al₂O₃ Phosphor.
- Sahu, G., Gour, A. S., & Chandrakar, R. K. (2017). Thermoluminescence and Optical Properties of Dy³⁺ Doped MgO Nanoparticles, Prepared by Solution Combustion Synthesis Method. *Journal of Pure Applied and Industrial Physics*, 7(4), 115-127.
- Saidu, A., Wagiran, H., Saeed, M. A., & Alajerami, Y. S. M. (2015). Thermoluminescence characteristics of zinc lithium borate glass activated with Cu⁺ (ZnO–Li₂O–B₂O₃: Cu⁺) for radiation dosimetry. *Journal of Radioanalytical and Nuclear Chemistry*, 304(2), 627-632. <https://doi.org/10.1007/s10967-014-3846-y>
- Yukihiro, E. G., Milliken, E. D., Oliveira, L. C., Orante-Barrón, V. R., Jacobsohn, L. G., & Blair, M. W. (2013). Systematic development of new thermoluminescence and optically stimulated luminescence materials. *Journal of Luminescence*, 133, 203-210. <https://doi.org/10.1016/j.jlumin.2011.12.018>
- Zorenko, Y., Gorbenko, V., Bilski, P., Twardak, A., Mandowska, E., Mandowski, A., & Sidletskiy, O. (2014). Comparative analysis of the scintillation and thermoluminescent properties of Ce-doped LSO and YSO crystals and films. *Optical materials*, 36(10), 1715-1719. <https://doi.org/10.1016/j.optmat.2014.02.002>

